

University of Warwick institutional repository: <http://go.warwick.ac.uk/wrap>

This paper is made available online in accordance with publisher policies. Please scroll down to view the document itself. Please refer to the repository record for this item and our policy information available from the repository home page for further information.

To see the final version of this paper please visit the publisher's website. Access to the published version may require a subscription.

Author(s): D.P. Woodruff

Article Title: The role of reconstruction in self-assembly of alkylthiolate monolayers on coinage metal surfaces

Year of publication: 2007

Link to published version:

<http://dx.doi.org/10.1016/j.apsusc.2007.07.081>

Publisher statement: Dp. P. Woodruff. (2007). The role of reconstruction in self-assembly of alkylthiolate monolayers on coinage metal surfaces. *Surface Science*, Vol. 254, pp. 76-81

The Role of Reconstruction in Self-Assembly of Alkylthiolate Monolayers on Coinage Metal Surfaces

D. P. Woodruff

Physics Department, University of Warwick, Coventry CV4 7AL, UK

Abstract

Through a combination of standard laboratory-based surface science methods, together with synchrotron radiation-based NIXSW (normal incidence X-ray standing wave) experiments, the interface structure of simple alkylthiolate ‘self-assembled monolayers’ on Cu(111), Ag(111) and Au(111) has been investigated over the last ~15 years. A key conclusion is that in all cases the adsorbate produces a substantial, density-lowering, reconstruction of the outermost metal layer, although the nature of these reconstructions is quite different on the three metals. The main results of these investigations are briefly reviewed and contrasted.

1. Introduction

Alkylthiolate ($\text{CH}_3(\text{CH}_2)_{n-1}\text{S}-$) adsorbates on coinage metal surfaces, and particularly the (111) faces, are perhaps the best-known and most widely exploited of self-assembled monolayers (SAMs) (e.g. [1, 2]). Despite this, the detailed nature of the interface structures has been largely unknown, the majority of the quantitative structural studies having been based on total energy calculations, rather than experiment. In a Warwick/Nottingham collaboration, mainly using the technique of normal incidence X-ray standing waves (NIXSW), but combined particularly with STM and medium energy ion scattering (MEIS), we have now established many of the key features of these interfaces, primarily through model studies of methylthiolate ($\text{CH}_3\text{S}-$) layers, but including some work on longer alkyl chains. In this short review the main results for the Cu(111), Ag(111) and Au(111) surfaces are brought together, and some general conclusions are reached. The results discussed here relate only to the so-called ‘standing-up’ ordered phases, and so far have not included detailed studies of the ‘striped’ or ‘lying-down’ phases seen, in particular, on Au(111) in which the alkane chains appear to lie essentially parallel to the surface.

Insofar as molecular ‘self-assembly’ implies a dominant role of intermolecular forces, there has been a tendency to assume that the metal surface is a rather passive spectator in this process, although the fact that many SAM structures are commensurate with the substrate clearly indicates that the corrugation of the adsorbate-substrate potential plays an important role. However, perhaps the most striking conclusion of our studies is clear evidence that the interaction of the thiols with all of these surfaces leads to major reconstruction of the outermost metal surface layer, although the nature of these reconstructions is quite different on the three metals. In view of this, each substrate will be considered separately, but a final section will include some general remarks. Before this, however, we briefly describe some of the main features of the methods used in these investigations. Note that while alkanethiol SAMs are most commonly produced by immersion in ethanolic solutions, almost all of our investigations have been conducted using gas-phase deposition, under ultra-high vacuum (UHV) ($\sqrt{3}\times\sqrt{3}$)R30° conditions,

onto single crystal surfaces prepared and characterised by standard UHV surface science methods

2. Experimental methods

Routine methods used in these investigations include STM, qualitative LEED (low energy electron diffraction) and XPS (X-ray photoelectron spectroscopy), although the latter method has been used with synchrotron radiation in both the soft and hard X-ray energy range, rather than using conventional laboratory sources. All of these methods are well known and need little explanation. STM and qualitative LEED provide information on lateral ordering of a surface, XPS provides information on adsorbate coverage and provides a spectral fingerprint of the 'chemical' state of adsorbates. The NIXSW and MEIS methods are less widely used, and deserve some brief explanation.

NIXSW [3, 4] is a minor variant of the more general XSW method in which one establishes an X-ray Bragg reflection in a crystalline substrate. The interference of the incident and diffracted beam leads to the formation of a standing wavefield, the intensity periodicity of which is equal to the interlayer spacing of the substrate scatterer planes. The fact that each substrate layer leads to significant scattering out of the crystal means that the X-ray penetration is finite (even in the absence of absorption) and this, in turn, leads to a finite range, in angle or photon energy (wavelength), of the high reflectivity and thus of the existence of the standing wave. Within this finite range the phase of the standing wavefield shifts relative to the scatterer planes in a systematic fashion by one half of the interlayer spacing. If one then studies the absorption of the X-rays at an atom in the solid or at the surface, the form of the variation of this absorption as one scans through the Bragg condition is characteristic of its location within the standing wave, and thus relative to the underlying crystal. The use of normal incidence to the scatterer planes allows the method to be applied to a wide range of materials because at this condition, a turning point in the Bragg condition, one is rather insensitive to crystal mosaicity which, at more general incidence conditions, can smear out the XSW absorption profile very severely for all but the most perfect crystals. Performing a NIXSW experiment using

scatterer planes parallel to the surface provides information on the height of the absorber atoms above the substrate scatterer planes, while additional measurements made with scatterer planes inclined to the surface provides information on the lateral registry. Triangulating these two or more measurements allows one to determine the absolute location of the absorber atom relative to the underlying crystal. This local atomic absorption can be monitored in a surface sensitive fashion through measurement of a core level photoemission signal (the XPS peak) or Auger electron emission resulting from refilling of the core hole.

MEIS [5] involves the scattering of typically 100 keV H^+ or He^+ ions from a surface. As in other ion scattering techniques, the elastic recoil energy loss in a binary collision of an incident ion with a near-surface atom allows one to identify the mass of this atom, by measuring the scattered ion energy spectrum. This elastic scattering leads to ‘shadow cones’ behind each scatterer atom – a region of space in which atoms are ‘hidden’ from the incident ion flux. In MEIS these shadow cones are narrow relative to typical interatomic spacings, but by aligning the incident beam along a low-index bulk crystallographic direction, one can ensure that only a small, and in principle integral, number of near-surface layers is illuminated. Because the scattering cross-sections are rather well known, accurate determinations of the exact number of layers contributing to the scattered ion signal can be made. Thus, if surface reconstruction occurs that leads to movement of surface atoms away from bulk-termination sites, these surface atoms no longer shadow sub-surface atoms and the scattered ion signal is enhanced. In this way MEIS provides a means of determining the number of displaced surface atoms in a surface reconstruction, and in some cases information on their exact locations.

3. Cu(111)

Although Cu is the least-studied of the coinage metal substrates for alkylthiolate SAMs, it is the one investigated first in our studies and so is described first. Room temperature exposure of this surface to either methanethiol, CH_3SH or dimethyldisulphide, CH_3S-SCH_3 , leads to the formation of a methylthiolate (CH_3S^-) layer, through thiol

deprotonation or S-S bond scission. This same surface reaction occurs at the Ag and Au surfaces. A key finding of a NIXSW [6] study of the Cu(111)/CH₃S- surface shows that the S headgroup atoms lies only 1.15 Å above the nearest extended Cu(111) bulk scatterer plane, a spacing that is too small to be compatible with any adsorption site on an unreconstructed surface, with any reasonable assumption regarding the Cu-S nearest-neighbour bonding distance. Essentially the same result was also found for an octylthiolate (n=8) SAM on this surface [7]. The clear implication of this result is that the outermost Cu atomic layer must reconstruct to a layer of lower atomic density, opening up larger hollow sites into which the S atoms may bond lower on the surface. This implication was supported by surface EXAFS (extended X-ray absorption spectroscopy) measurements of the S-Cu bondlength and bond angle [6].

Initially, it was assumed that this reconstructed layer would have the same hexagonal symmetry as the substrate [8], but later STM work (on both methylthiolate [9] and octylthiolate [10] layers) showed that in fact the reconstructed layer has near-square symmetry, the S headgroup atom thus occupying 4-fold coordinated hollow sites within this layer. This type of pseudo-(100) reconstruction of an fcc (111) surface has been observed for a number of atomic adsorption systems, and indeed even occurs on some fcc (110) surfaces [11], but this seems to be the first example of a molecular adsorbate having this effect. This structure is illustrated in Fig. 1 and has been further supported by MEIS measurements that confirm the number of displaced Cu atoms in the outermost layer is consistent with this model [12], with just one reconstructed pseudo-(100) layer. The rationale for this type of reconstruction is thought to be that the four-fold coordinated site on a near-square surface mesh structure is so favourable that this reconstruction has a lower energy than adsorption on the unreconstructed surface, despite the strain energy associated with the interface between the outermost (111) (or (110)) substrate layer and the pseudo-(100) reconstructed layer.

In general, the adsorption systems showing pseudo-(100) reconstructions are all ones in which a c(2x2) structure, with hollow site adsorption, is found when the same adsorbate is adsorbed onto the (100) surface. In these cases, the lateral dimensions of the pseudo-

(100) reconstructed layer on the (111) surface is very similar to that of the (100) surface. However, the case of methylthiolate on Cu(111) appears to be an exception – the lateral periodicity of the pseudo-(100) layer is almost 15% larger than that of the (100) surface. Methylthiolate does occupy the 4-fold coordinated hollow site on Cu(100) [13, 14], but it does not form a well-ordered $c(2 \times 2)$ phase. A lower coverage (2×2) phase is first formed, but at higher coverage a $c(2 \times 6)$ phase is seen; this phase is thought to have local $c(2 \times 2)$, but to be buckled due to compressive surface stress [15]. The fact that $c(2 \times 2)$ ordering of the thiolate on the pseudo-(100) reconstructed surface on Cu(111) is accompanied by a lateral expansion of the layer is thus not too surprising. Indeed, even on this relaxed reconstructed surface, the lateral intermolecular spacing is only 4.12 Å which, as we shall see below, is short in comparison to the main SAM phases on Ag(111) and Au(111). It is presumably for this reason that this particular case of a pseudo-(100) reconstructed layer the lateral dimensions are significantly larger than on the (100) surface itself.

3. Ag(111)

On Ag(111) it is well established that methylthiolate forms an ordered $(\sqrt{7} \times \sqrt{7})R19.1^\circ$ ordered phase from the LEED pattern recorded in an early spectroscopic study of this system [16]. Atomic S also produces a surface phase with this same unit mesh, but in this case the structure has been attributed to multilayers of f-cubic $\text{Ag}_2\text{S}(111)$ which has a very close match in lattice parameter [17]. One feature of this bulk sulphide structure is that within the $(\sqrt{7} \times \sqrt{7})$ unit mesh are three equally-spaced S atoms, thus on a submesh with a periodicity of $\sqrt{7/3}$ times that of the Ag(111) substrate, corresponding to a value of 4.41 Å (see Fig. 2, left). This similarity has led to the suggestion that methylthiolate species have this same submesh, although until recently all discussions have failed to consider any specific role of reconstruction of the Ag(111) surface. One interesting feature of this model is that the full three-fold rotational symmetry of the system can be retained if the lateral registry of the thiolate overlayer is such that the three inequivalent molecules occupy atop and hcp and fcc hollow sites (the latter two sites being atop second and third layer Ag atoms respectively). In fact a key finding of an early STM study of this phase was the observation, under different tip conditions, of either the $\sqrt{7}$ or

the $\sqrt{7/3}$ periodicity [18], but more recently we have reported images that show both periodicities [19], all observed atomic protrusions being on a $\sqrt{7/3}$ mesh, but with one third of these, on a regular $\sqrt{7}$ mesh, being slightly higher than the others. Qualitatively, at least, this observation is entirely consistent with the simple overlayer model described above, as the thiolate species in the atop site would be expected to be significantly higher above the surface than those in the hollow sites. However, the height difference seen in STM is less than half the value one would expect for reasonable values of the S-Ag bonding distance, so while STM is known to be an unreliable probe of height differences due to electronic effects, the discrepancy does seem significant. Clear evidence that this simple overlayer model cannot be correct, however, comes again from NIXSW measurements [20] that, as in the case of Cu(111), yield S-Ag interlayer spacings too small to be consistent with any combination of pure overlayer sites. Here too, therefore, the implication is that there must be a reconstructed, lower-density, outermost Ag layer providing enlarged hollow sites for thiolate adsorption at a lower height above the surface.

A quantitative analysis of the NIXSW data from the Ag(111) ($\sqrt{7}\times\sqrt{7}$)R19.1°-CH₃S-surface, supported by the STM investigation, led to the specific structural model shown in fig. 2, right. Unlike the case of Cu(111), the STM data shows clearly that the reconstructed Ag layer on Ag(111) must retain the hexagonal symmetry of the substrate, rather than the near-square symmetry of a pseudo-(100) reconstruction, and the specific model that best fits the data involves a reconstructed layer comprising only 3/7 ML of Ag atoms, the layer same density as that of the thiolate species. This reconstructed Ag layer density has also been shown to be compatible with MEIS measurements [21]. In this model, all three-fold coordinated hollow sites within this layer are thus occupied by a S head-group atom, and the low Ag density means that the hollow sites are very open and the S atoms can occupy sites quite low above the surface. The symmetric geometry in which these S head-group atoms occupy atop, hcp hollow and fcc hollow sites relative the underlying outermost unreconstructed Ag(111) layer is retained in the model. The thiolate intermolecular lateral spacing in this structure is 4.41 Å, significantly larger than on the reconstructed Cu(111) surface.

NIXSW measurements on octylthiolate [22] and pentylthiolate (n=5) [23] also indicate similar S/Ag interlayer spacings that must imply a similar reconstruction. In the case of the longer-chain alkanethiolates, however, there is evidence that the thiolate lateral spacing is *not* commensurate with the substrate. In particular, an investigation of the n=18 thiolate on Ag(111) using X-ray diffraction low-energy He atom diffraction led to the conclusion that for this species an ordered phase having two rotational domains similar to that of the $(\sqrt{7}\times\sqrt{7})R19.1^\circ$ structure is formed, but the lateral periodicity is ~6% larger than this commensurate structure [24]. Subsequently, one STM study of decanethiolate (n=10) on Ag(111) [25] came to a similar conclusion, while most recently our own STM and LEED measurements on the pentylthiolate (n=5) layer also indicated an enlarged, incommensurate, surface unit mesh [26]. As remarked above, our NIXSW measurements on the pentylthiolate layer indicate that a similar Ag surface reconstruction to that shown in Fig. 2 (right) must occur, although with an enlarged (incommensurate) surface unit mesh. The implication of this result is that while the intermolecular interactions in the methylthiolate layer are sufficiently weak to allow the corrugation of the substrate interaction potential to dominate, producing a commensurate structure, this intermolecular interaction in the longer alkane chains is sufficient to overcome this corrugation and determine more directly the size of the surface unit mesh of the SAM.

4. Au(111)

Alkylthiolate layers on Au(111) are surely the most extensively studied of all SAM systems, and there has long been the implicit assumption that the thiolates bond to an ideally-terminated Au(111) substrate layer. Perhaps the one historical piece of evidence that this might not be the case is the widely-reported observation of single atomic layer deep pits in the surface with STM, indicating significant movement of Au surface atoms in the formation of the SAMs. However, the clean Au(111) surface is known to display a ‘herring-bone’ reconstruction in which the outermost layer adopts a hexagonal close packing of higher density than the underlying substrate, and quite low coverages of thiolate are known to destroy this reconstruction, leading to a more ideal (1x1) surface

termination. This unreconstruction, therefore, is itself a source of substantial atomic movement, and could possibly be the cause of these pits.

More recently, however, two independent determinations of the local adsorption geometry of methylthiolate on Au(111) in a $(\sqrt{3}\times\sqrt{3})R30^\circ$ ordered phase by wholly different methods, namely photoelectron diffraction [27] and NIXSW [28], led to some doubt regarding this perspective. Specifically, these two investigations found that the S headgroup atom occupies a site directly atop surface Au atoms, whereas the results of many theoretical total energy calculations had concluded that the favoured adsorption site was either a three-fold coordinated hollow, a two-fold coordinated bridge site, or a site somewhere between these two positions. This stark contrast between the experimental and theoretical results would appear to imply one of two things: either the theoretical methods (mainly density functional theory – DFT) in some way consistently fails for this adsorption system (as is known to occur, for example, in determining the preferred adsorption site of CO on Pt(111) [29]), or none of the theoretical treatments had actually tested the correct structural model. The most obvious way in which the latter situation may arise is if the thiolate adsorption induces a surface reconstruction of the Au(111) surface. In fact, one DFT study of this system [30] did investigate two possible reconstruction models, the ‘honeycomb’ (HC) model, in which 1/3 of the surface layer Au atoms are missing (an ordered vacancy model), and the ‘inverse honeycomb’ (IHC) model, in which 2/3 of the surface Au atoms are missing, or equivalently, the surface comprises 1/3 ML of Au adatoms. Interestingly, these authors found the lowest energy geometry for the IHC model was with adsorption in atop sites, but also found that adsorption in or near bridge sites on the IHC model was the lowest energy structure.

One notable feature of the ‘standing-up’ phases of alkylthiolate SAMs on Au(111) is the common observation of two distinct ordered phases, one having the $(\sqrt{3}\times\sqrt{3})R30^\circ$ mentioned above, the other having a $(3\times 2\sqrt{3})$ rect. mesh (sometimes referred to as a $c(4\times 2)$ supermesh of the basic $(\sqrt{3}\times\sqrt{3})R30^\circ$ structure). These two phases are thought to have the same coverage of 0.33 ML, but whereas in the $(\sqrt{3}\times\sqrt{3})R30^\circ$ mesh all molecules must have locally identical adsorption geometries (one molecule per surface unit mesh),

in the $(3 \times 2\sqrt{3})$ rect. mesh at least two, and up to four distinct sites must be occupied. Experiments indicate, however, that these phases generally coexist, and that interconversion is facile (e.g. by modified annealing or even the passage of a STM tip), implying that their energies must be extremely similar. In an attempt to understand these different structures, we have conducted NIXSW investigation of several different alkylthiolate species ($n=1,4,6,8$) on Au(111) [31]. The results revealed a distinct difference between short-chain thioliates in the $(\sqrt{3} \times \sqrt{3})R30^\circ$ phase and longer-chain thioliates in a mixture of the two phases. In particular, while the height of the S headgroup atoms above the underlying substrate appears to be identical, the lateral registry differs. As remarked above, the short-chain thioliates in the $(\sqrt{3} \times \sqrt{3})R30^\circ$ phase are found to adopt atop sites. However, triangulation of two different NIXSW measurements for the mixed-phase longer-chain thioliates indicates a mixture of two sites are occupied, one of which is the same atop site, but the second site is initially identified as the fcc hollow site. What is clear, however, is that S atoms cannot occupy atop and hollow sites at the same height above the underlying substrate, so this initial conclusion appears to be fundamentally inconsistent. The solution to this dilemma is to assume that *all* S headgroup atoms occupy sites atop Au adatoms on the surface, some of which are in fcc hollows while others are in hcp hollows. S atoms atop fcc adatoms will triangulate to an atop registry relative to the substrate (the Au adatom occupying a bulk termination site) but those S atoms atop hcp Au adatoms will triangulate to an apparent fcc hollow. This is because these S atoms lie directly above an Au atom three Au(111) layer spacings below, exactly as in a fcc hollow. The resulting model, with all S atoms lying atop Au atoms in hollow sites, ensures, of course, that they are all at the same height above the underlying substrate.

This structural model implies that a complete re-evaluation of the nature of self-assembly is required to understand alkylthiolate SAMs on Au(111). In particular, the self-assembly involves the organisation of Au-adatom-thiolate moieties, and not simply thiolate species, and the nature of the substrate corrugation potential in these two cases is quite different. Although the NIXSW results provide only indirect evidence of the Au adatom model, it is interesting to note that recent low temperature STM has provided direct evidence of

thiolate/adatom species on the Au(111) surface [32]. Moreover, recent total energy calculations of ethylthiolate bonded atop Au adatoms on Au(111) [33] indicate that the energy of the fcc and hcp adatom sites is almost identical, and that the barrier to diffusion between them is very small, making transformation between these sites facile.

Fig. 3 shows the structural model implied by this analysis for the $(\sqrt{3}\times\sqrt{3})R30^\circ$ thiolate phase (based on S headgroup atoms atop Au adatoms in fcc hollow sites) together with one possible structural model for the $(3\times 2\sqrt{3})$ rect. phase, in this case assuming that within this larger unit mesh half of the Au adatoms are in fcc hollows, and half in hcp hollows. Notice that one feature of any model based on a mixture of fcc and hcp adatom sites is that some of the local S-S interatomic distances (and hence the intermolecular distances) are reduced from the value of 4.99 Å in the $(\sqrt{3}\times\sqrt{3})R30^\circ$ phase to only 3.33 Å. This value is even shorter than the 4.12 Å seen in the reconstructed Cu(111) surface, and suggest that some modification of the exact model of fig. 3 may be required. In this regard, however, we note that the NIXSW data would differ little if the S atoms were displaced laterally from the ideal atop sites by ~ 0.3 Å, so a local intermolecular distance similar to that on the Cu surface could be consistent with the experimental data.

5. General remarks

A key finding of our investigations of these alkylthiolate layers on Cu(111), Ag(111) and Au(111) is that in all cases adsorbate-induced reconstruction of the surface occurs, with major changes in the density of the outermost metal atom layer. This is clearly of profound significance to a detailed understanding of the balance between the intermolecular forces, and the corrugation of the molecule-substrate potential, that determines the nature of the ordering – the self-assembly. Clearly, theoretical total energy calculations can help to elucidate this issue, but currently almost all such calculations have been performed assuming that no reconstruction occurs. Of course, the incommensurate or large surface mesh structures associated with the Ag(111) and Cu(111) surface phases presents a substantial challenge for such calculations, although there is certainly scope to perform calculations on structures significantly more relevant

to the true structures than have been conducted so far. In the case of Au(111), smaller commensurate surface mesh phases do occur, but a fuller analysis of the influence of reconstruction and the role of Au adatoms needs to be addressed. Of course, the full range of thiol/Au(111) phenomena is broad and complex, and there is also a need for further experiments, here too particularly trying to understand the role of Au adatoms in the formation of these structures.

Acknowledgements

The work described here is the result of a long-term collaboration with Professor Rob Jones at the University of Nottingham, involving the considerable effort of many research students and postdoctoral researchers, both at Warwick and Nottingham, whose names appear in many of the cited papers. The role of all of these collaborators is gratefully acknowledged, as is the award of synchrotron radiation beamtime at the Synchrotron Radiation Source (SRS) at Daresbury Laboratory, allowing many of the key experiments to be performed.

Figure Captions

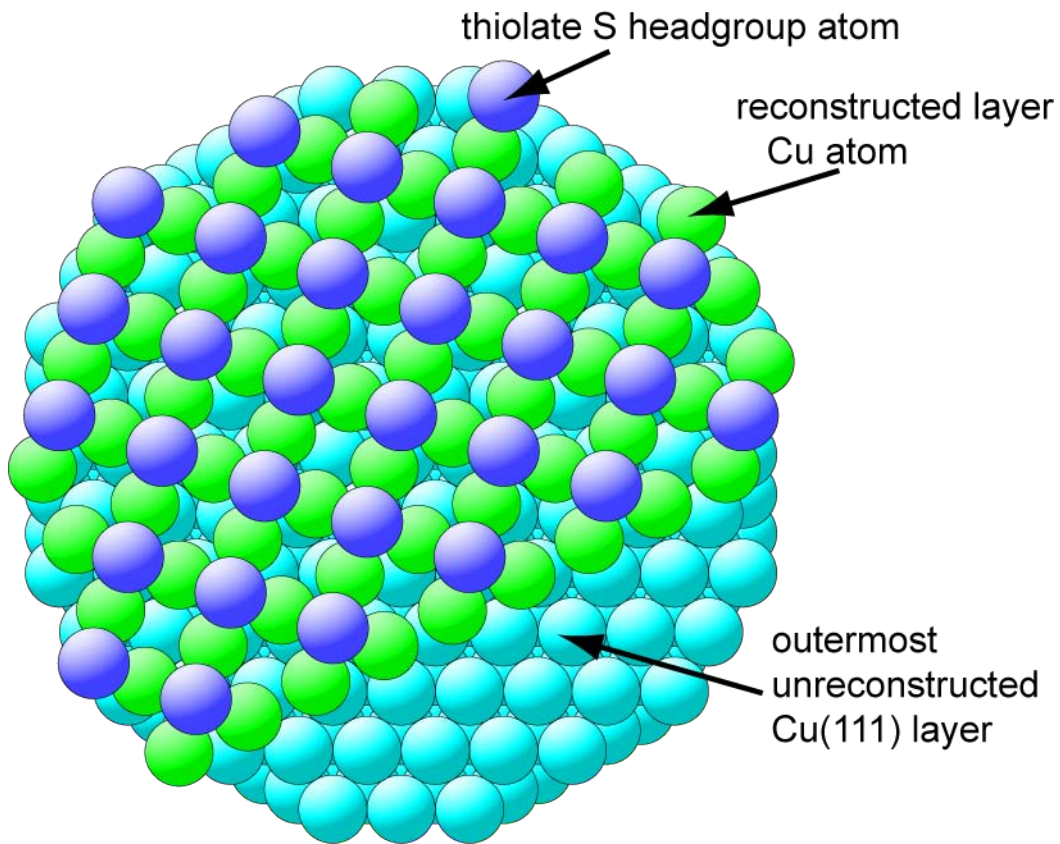


Fig. 1 Plan view of schematic diagram of the pseudo-(100) reconstruction of Cu(111) formed by an adsorbed layer of methylthiolate or octylthiolate at room temperature. The overlayer has been omitted from the lower right-hand side of the diagram to expose the underlying Cu(111) substrate. Only the S headgroup atoms of the thiolate are shown as the smallest spheres.

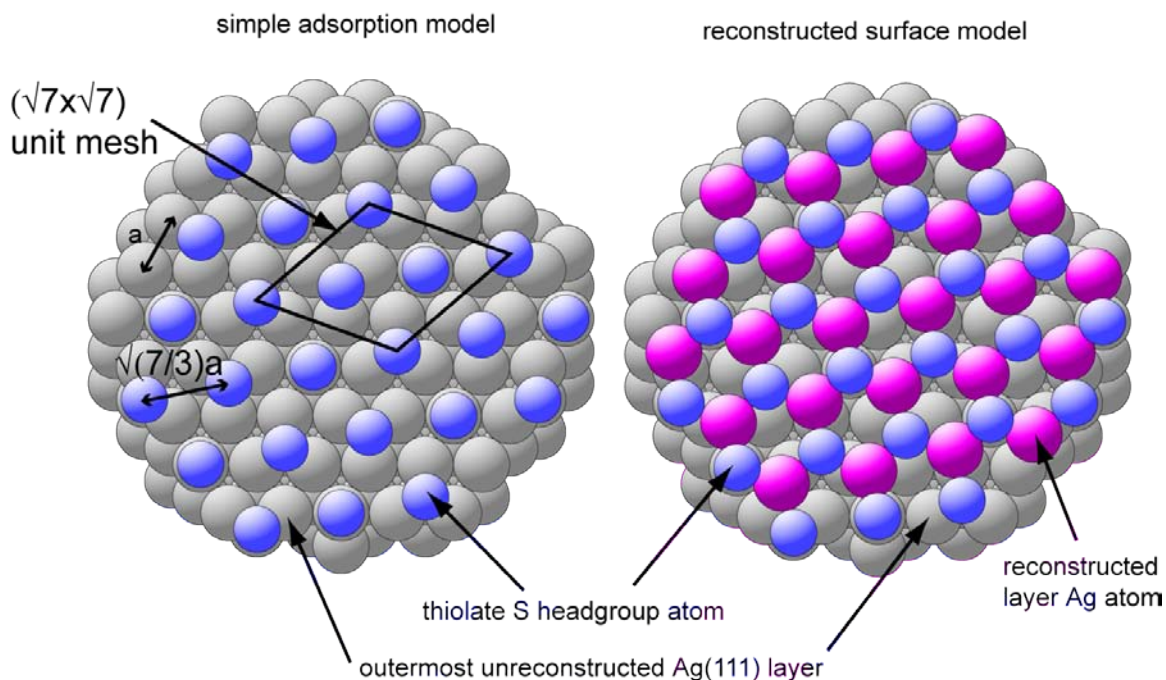


Fig. 2 Plan view of the Ag(111) surface showing the optimised (reconstructed surface) structural model for the $(\sqrt{7} \times \sqrt{7})R19.1^\circ\text{-CH}_3\text{S-}$ phase on the right. On the left is shown the basic starting model (not including Ag surface reconstruction) described previously in the literature, and based on the early study of the $(\sqrt{7} \times \sqrt{7})R19.1^\circ\text{-S}$ surface phase. Only the S headgroup atoms of the thiolate are shown as the smallest spheres.

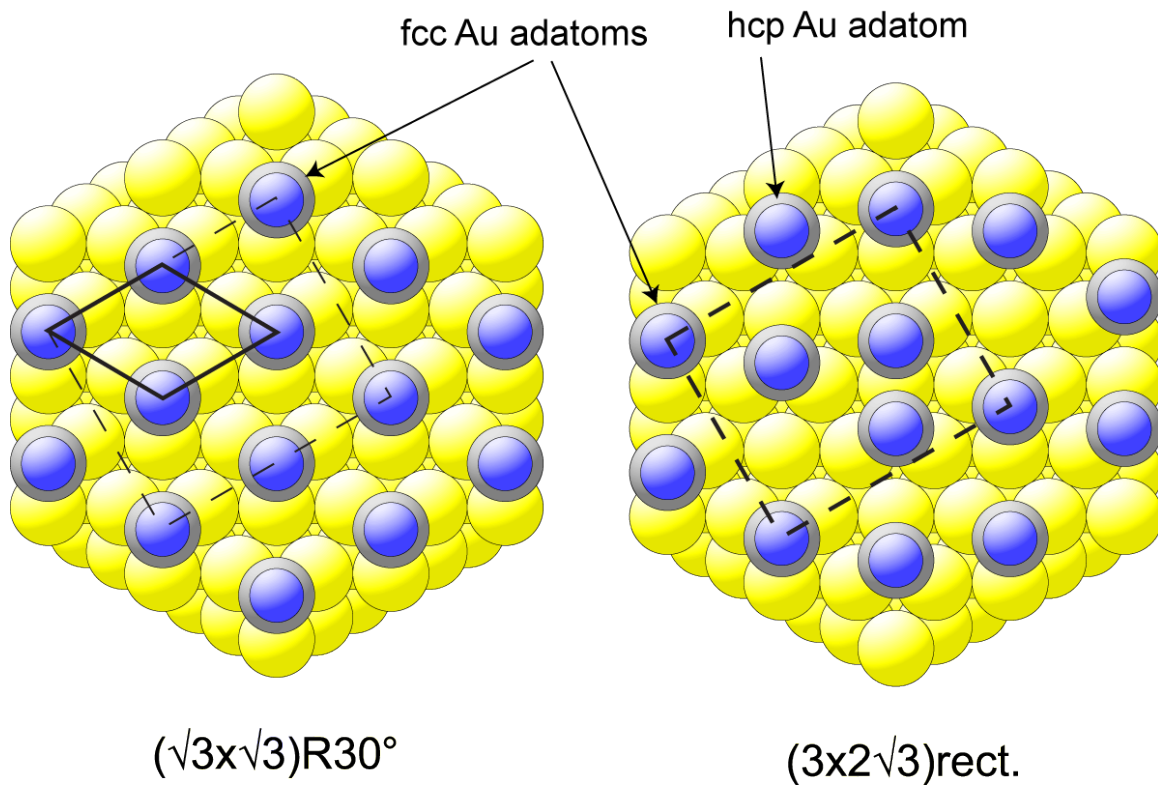


Fig. 3 Plan view of the Au(111) surface showing the structural model for the $(\sqrt{3}\times\sqrt{3})R30^\circ$ thiolate phase (based on S headgroup atoms atop Au adatoms in fcc hollow sites) and one possible structural model for the $(3\times 2\sqrt{3})\text{rect.}$ phase., based on a 1:1 ratio of fcc:hcp adatom sites. Only the S headgroup atoms of the thiolate are shown as the smallest spheres. The $(\sqrt{3}\times\sqrt{3})R30^\circ$ unit mesh is shown in bold lines, the $(3\times 2\sqrt{3})\text{rect.}$ unit mesh is shown in dashed lines.

References

- 1 F. Schreiber, *Prog. Surf. Sci.* 65 (2000) 151
- 2 A. Ulman, *Chem. Rev.* 96 (1996) 1533
- 3 D. P. Woodruff, *Prog. Surf. Sci.* 57 (1998) 1
- 4 D. P. Woodruff, *Rep. Prog. Phys.* 68 (2005) 743
- 5 J. F. van der Veen, *Surf. Sci. Rep.* 5 (1985) 199
- 6 N. P. Prince, D. L. Seymour, D. P. Woodruff, R. G. Jones, W. Walter, *Surf. Sci.* 215 (1989) 566
- 7 H. Rieley, G. K. Kendall, A. Chan, R. G. Jones, J. Lüdecke, D. P. Woodruff, B. C. C. Cowie, *Surf. Sci.* 392 (1997) 143
- 8 N. P. Prince, M. J. Ashwin, D. P. Woodruff, N. K. Singh, W. Walter, R. G. Jones, *Faraday Discuss. Chem. Soc.* 89 (1990) 301
- 9 S. M. Driver, D. P. Woodruff, *Surf. Sci.* 457 (2000) 11
- 10 S. M. Driver, D. P. Woodruff, *Langmuir*, 16 (2000) 6693
- 11 D. P. Woodruff, *J. Phys.: Condens. Matter* 6 (1994) 6067
- 12 G. S. Parkinson, M.A. Muñoz-Márquez, P.D. Quinn, M. Gladys, D.P. Woodruff, P. Bailey, T.C.Q. Noakes, *Surf. Sci.* 598 (2005) 209
- 13 A. Imanishi, S. Takanaka, Y. Yokoyama, Y. Kitajima, T. Ohta *J. Physique IV* 7 C2 (1997) 701
- 14 M. S. Karriaper, C. Fisher, D. P. Woodruff, B. C. C. Cowie, R. G. Jones, *J. Phys.: Condens. Matter* 12 (2000) 2153
- 15 S. M. Driver, D. P. Woodruff, *Surf. Sci.* 488 (2001) 207
- 16 A. L. Harris, L. Rothberg, L. H. Dubois, N. J. Levinos, L. Dhar, *Phys. Rev. Lett.* 64 (1990) 2086.
- 17 K. Schwaha, N. D. Spencer, R. M. Lambert, *Surf. Sci.* 81 (1979) 273.
- 18 R. Heinz, J. P. Rabe *Langmuir* 11 (1995) 506.
- 19 Miao Yu, S.M. Driver, D.P. Woodruff, *Langmuir* 21 (2005) 7285.
- 20 Miao Yu, D.P. Woodruff, N. Bovet, C.J. Satterley, K. Lovelock, Robert G. Jones, V. Dhanak, *J. Phys. Chem. B* 110 (2006) 2164

-
- 21 G. S. Parkinson, A. Hentz, P. D. Quinn, A. J. Window, D. P. Woodruff, P. Bailey, T. C. Q. Noakes, *Surf. Sci.* in press
- 22 H. Rieley, G. K. Kendall, R. G. Jones, D. P. Woodruff, *Langmuir*, 15 (1999) 8856
- 23 Miao Yu *et al.*, to be published
- 24 P. Fenter, P. Eisenberger, J. Li, N. Camillone III, S. Bernasek, G. Scoles, T. A. Ramanarayanan, K. S. Liang, *Langmuir*, 7 (1991) 2013
- 25 A. Dhirani, M. A. Hines, A. J. Fisher, O. Ismail, P. Guyot-Sionnest, *Langmuir*, 11 (1995) 2609
- 26 Miao Yu, D.P. Woodruff, Christopher J. Satterley, Robert G. Jones, V. R. Dhanak, to be published
- 27 H. Kondoh, M. Iwasaki, T. Shimada, K. Amemiya, T. Yokohama, T. Ohta, M. Shimomura and K. Kono, *Phys. Rev. Lett.* 90 (2003) 066102-1
- 28 M.G. Roper, M.P. Skegg, C.J. Fisher, J.J. Lee, V. R. Dhanak, D.P. Woodruff, R. G. Jones, *Chem. Phys. Lett.* 389 (2004) 87
- 29 P. Feibelman, B. Hammer, J. K. Nørskov, F. Wagner, M. Scheffler, R. Stumpf, R. Watwe, J. Dumesic, *J. Phys. Chem. B.* 105 (2001) 4018
- 30 L. M. Molina, B. Hammer, *Chem. Phys. Lett.* 360 (2002) 264
- 31 Miao Yu, N. Bovet, Christopher J. Satterley, S. Bengiό, Kevin R. J. Lovelock, P. K. Milligan, Robert G. Jones, D. P. Woodruff, V. Dhanak, *Phys. Rev. Lett.* 97 (2006) 166102
- 32 P. Maksymovych, D. S. Sorescu, J. T. Yates, Jr. *Phys. Rev. Lett.* 97 (2006) 146103
- 33 F. P. Cometto, P. Paredes-Olivera, V. A. Macagno, E. M. Patrito, *J. Phys. Chem. B* 105 (2005) 21737